


LETTER

Incorporating pressure–volume traits into the leaf economics spectrum

Miquel Nadal^{1,2}  | María J. Clemente-Moreno² | Alicia V. Perera-Castro^{2,3} |
Margalida Roig-Oliver² | Yusuke Onoda⁴ | Javier Gulías² | Jaume Flexas²

¹Departamento de Sistemas Agrícolas, Forestales y Medio Ambiente, Centro de Investigación y Tecnología Agroalimentaria de Aragón (CITA), Zaragoza, Spain

²Research Group on Plant Biology under Mediterranean Conditions, Institut d'Investigacions Agroambientals i d'Economia de l'Aigua (INAGEA) – Universitat de les Illes Balears (UIB), Palma, Spain

³Department of Botany, Ecology and Plant Physiology, Universidad de La Laguna (ULL), La Laguna, Spain

⁴Graduate School of Agriculture, Kyoto University, Kyoto, Japan

Correspondence

Miquel Nadal, Departamento de Sistemas Agrícolas, Forestales y Medio Ambiente, Centro de Investigación y Tecnología Agroalimentaria de Aragón (CITA), Avda. Montañana 930, Zaragoza 50059, Spain. Email: m.n.nadal92@gmail.com

Funding information

European Regional Development Fund, Grant/Award Number: PGC2018-093824-B-C41; European Social Fund, Grant/Award Number: BES-2015-072578; Japan Society for the Promotion of Science, Grant/Award Number: KAKENHI #21H02564; Ministerio de Ciencia e Innovación, Grant/Award Number: FJC2020-043902-I; Ministerio de Ciencia, Innovación y Universidades, Grant/Award Number: PGC2018-093824-B-C41; Ministerio de Economía y Competitividad, Grant/Award Number: BES-2015-072578 and FPU16/01544; Ministerio de Educación, Cultura y Deporte, Grant/Award Number: FPU-02054

Editor: Josep Penuelas

Abstract

In recent years, attempts have been made in linking pressure–volume parameters and the leaf economics spectrum to expand our knowledge of the interrelationships among leaf traits. We provide theoretical and empirical evidence for the coordination of the turgor loss point and associated traits with net CO₂ assimilation (A_n) and leaf mass per area (LMA). We measured gas exchange, pressure–volume curves and leaf structure in 45 ferns and angiosperms, and explored the anatomical and chemical basis of the key traits. We propose that the coordination observed between mass-based A_n , capacitance and the turgor loss point (π_{tlp}) emerges from their shared link with leaf density (one of the components of LMA) and, specially, leaf saturated water content (LSWC), which in turn relates to cell size and nitrogen and carbon content. Thus, considering the components of LMA and LSWC in ecophysiological studies can provide a broader perspective on leaf structure and function.

KEYWORDS

capacitance, leaf economics spectrum, leaf structure, leaf water content, photosynthesis, pressure–volume, turgor loss point

INTRODUCTION

The leaf economics spectrum (LES) provides a general framework for carbon economics and nutrient use in leaves among all plant groups and biomes (Wright et al., 2004), being net CO₂ assimilation (A_n), dark respiration rate (R_d), leaf mass per area (LMA), nutrient content (N and P) and leaf lifespan (LL) the central traits constituting a common axis of variation. The coordinated shifts of these traits drive carbon

and nutrient use-efficiency in leaves, and they are integrated into a fast versus slow continuum of strategies and processes at the plant and community levels (Cornwell et al., 2008; Díaz et al., 2016; Reich, 2014; Westoby & Wright, 2006). Since the LES was established, an increasing number of studies have explored its coordination with other aspects of leaf physiology, including hydraulics and venation architecture (Blonder et al., 2011; Sack et al., 2013), mechanical properties (He et al., 2019; Onoda et al., 2011), anatomy, composition,

This is an open access article under the terms of the [Creative Commons Attribution-NonCommercial-NoDerivs](https://creativecommons.org/licenses/by-nc-nd/4.0/) License, which permits use and distribution in any medium, provided the original work is properly cited, the use is non-commercial and no modifications or adaptations are made.

© 2023 The Authors. *Ecology Letters* published by John Wiley & Sons Ltd.

and nitrogen allocation (Hikosaka & Shigeno, 2009; John et al., 2017; Onoda et al., 2017), and CO₂ diffusion inside leaves (Flexas et al., 2008; Niinemets et al., 2009). These efforts have contributed to disentangle the interrelationships among leaf traits and to establish the mechanistic basis of the LES (Flexas et al., 2013; Onoda et al., 2017; Shipley et al., 2006). In addition, the availability of extensive databases, being TRY the primary example (Kattge et al., 2011, 2020), has made possible for ecologists to explore the variability and responses of leaf traits at a much larger scale (e.g. Atkin et al., 2015; He et al., 2020; Xing et al., 2021). However, there is still a need to integrate additional aspects of leaf physiology into this growing network of traits, and to do so with precise understanding of the exact nature of their association. In particular, the inclusion of traits reflecting water stress tolerance would greatly help in discerning critical trade-offs at the leaf level (Reich, 2014), and in integrating the LES into upscaling models of vegetation in a changing environment (Díaz et al., 2016; van Bodegom et al., 2014). In this sense, here we aim to explore the coordination of photosynthesis and structure with pressure–volume (PV) traits, which reflect plant strategies in relation to water availability (Bartlett, Scoffoni, et al., 2012; Xiong & Nadal, 2020; Zhu et al., 2018).

PV traits describe water relations in leaves, that is, the interplay between water potential (pressure and osmotic potential) and water content and (symplast) volume, averaged across all tissues and cells within the leaf (Tyree & Jarvis, 1982). Among the PV traits (listed in Table 1), the osmotic potential at the turgor loss point (π_{tlp}) is considered to be a key indicator of drought tolerance. Lower π_{tlp} occurs in plants from drier habitats (Bartlett, Scoffoni, et al., 2012; Lenz et al., 2006; Zhu et al., 2018), and correlates with other indices of water stress tolerance, including minimum water potential experienced in the field (Zhu et al., 2018), stomatal and hydraulic decline (Bartlett et al., 2016; Martin-StPaul et al., 2017), and recovery after dehydration (John et al., 2018). π_{tlp} is strongly related to the osmotic potential at full turgor (π_0) and, to a lesser extent, the bulk modulus of elasticity (ϵ ; Bartlett, Scoffoni, et al., 2012). Elasticity influences the relative water content at the turgor loss point (RWC_{tlp} ; Bartlett, Scoffoni, et al., 2012; Perera-Castro et al., 2020) and is usually associated with sclerophylly (Read et al., 2006; Salleo & Nardini, 2000). The tissue components and/or cell arrangements that may determine ϵ are still unclear, although tissue density and cell wall thickness have been proposed to influence ϵ (Niinemets, 2001; Peguero-Pina, Sancho-Knapik, et al., 2017). Leaf capacitance, defined as the change in water content for a given range of water potential, has received less attention despite its potential role as a buffer protecting against rapid changes in water potential, especially in leaves with high transpiration capacity (Sack & Tyree, 2005; Xiong

& Nadal, 2020). Capacitance is also associated with the kinetics of stomatal closure and with dehydration tolerance (see Xiong & Nadal, 2020). Recently, some studies have explored the potential coordination between these parameters and the LES traits. Most notably, the extensive meta-analysis performed by Zhu et al. (2018) showed a negative correlation between π_{tlp} and LMA and, to a lesser extent, mass-based A_n ($A_{n,\text{mass}}$), thus providing a first hint to the potential coordination of carbon and water economics. However, the relationship between LMA and π_{tlp} reported by Zhu et al. (2018) is relatively weak and is elusive when considering specific plant groups and/or ecosystems (Májeková et al., 2021; Maréchaux et al., 2020). On the other hand, Nadal et al. (2018) described the relationship of area-based A_n ($A_{n,\text{area}}$) and ϵ , although it is not clear if this relationship emerges through a common mechanistic basis, such as mesophyll cell wall thickness (Peguero-Pina, Sancho-Knapik, et al., 2017), or due to the necessity of increased capacitance in leaves subjected to high transpiration (Blackman & Brodribb, 2011; Sack et al., 2003; Xiong & Nadal, 2020). These studies also highlight the need to consider area- and mass-based expressions of parameters, not only due to their distinct ecophysiological significance (Onoda & Wright, 2018; Westoby et al., 2013), but also due to the mathematical pitfalls associated with comparing non-independent variables (Lloyd et al., 2013; Osnas et al., 2013).

In the present study, we aim to provide theoretical and empirical evidence for the coordination between photosynthesis, structure and PV traits. First, a set of relatively simple equations provides the theoretical framework for the analysis and interpretation of the leaf traits included in the present study (Table 1, Box 1). Our approach is based on the distinct consideration of area- and mass-based traits, and the separation of LMA into its two components, leaf thickness (LT) and density (LD). This allows relating LD to the water content of leaves (Pyankov et al., 1999; Vile et al., 2005) and thus π_{tlp} and capacitance following Bartlett, Scoffoni, and Sack (2012). Considering LT and LD independently is not a novel approach; indeed, a number of studies have linked either thickness or density to a given variable to avoid the potential confounding effects of LMA (Hodgson et al., 2011; Kitajima & Poorter, 2010; Niinemets, 1999; Witkowski & Lamont, 1991). Here we hypothesise that the water content of leaves and LD (not LT) play a central role in leaf trait relationships through their effects on $A_{n,\text{mass}}$, π_0 and leaf mass-specific capacitance at full turgor ($C_{\text{ft,mass}}^*$). To test this hypothesis, we performed gas exchange, leaf structure and PV measurements in 45 ferns and angiosperms to explore the relationships described in Box 1. In addition, we also analysed leaf anatomy, carbon and nitrogen content and cell wall composition in the subset of the species from Nadal et al. (2018) to further explore the anatomical and

TABLE 1 Main photosynthetic, structural and pressure–volume traits included in the study. See [Box 1](#) for their derivation and the proposed theoretical framework describing their coordination.

Parameter	Definition	Units	Significance	Reference
<i>Photosynthesis</i>				
$A_{n, \text{mass}}$	Net CO ₂ assimilation rate per dry mass	nmol g ⁻¹ s ⁻¹	Photosynthetic ‘return’ per unit of dry mass ‘investment’; negatively related to leaf lifespan; represents the carbon economics of leaves	Westoby et al. (2013); Onoda and Wright (2018)
$A_{n, \text{area}}$	Net CO ₂ assimilation rate per area	μmol m ⁻² s ⁻¹	Light-saturated photosynthesis, associated to the light interception of leaves (flux per unit area); determined by anatomical features and N investment	Westoby et al. (2013); Onoda et al. (2017); Flexas et al. (2021)
<i>Structure</i>				
LMA	Leaf mass per area	g m ⁻²	Construction cost per unit of light-intercepting leaf area; related to plant growth rate	Poorter et al. (2009); Onoda and Wright (2018)
LT	Leaf thickness	mm	Component of LMA representing the investment on cell layers on the <i>z</i> axis for light interception	Niinemets (2001); Poorter et al. (2009)
LD	Leaf density	g cm ⁻³	Component of LMA representing the air and different tissue fractions; related to leaf robustness and water stress tolerance	Niinemets (2001); Poorter et al. (2009)
<i>Pressure–volume traits</i>				
LSWC	Leaf saturated water content	g g ⁻¹	Total amount of water at full saturation per dry mass (inverse of leaf dry matter content, LDMC); related to LD and stress response	Vile et al. (2005); Hodgson et al. (2011)
π_{tlp}	Osmotic potential at the turgor loss point	MPa	Potential at the turgor loss or wilting point; drought tolerance indicator; more negative values related to drier habitats	Bartlett, Scoffoni, et al. (2012); Zhu et al. (2018)
π_0	Osmotic potential at full turgor	MPa	Solute concentration in cells at full saturation; strongly related to π_{tlp} ; decreases under drought (osmotic adjustment)	Bartlett, Scoffoni, et al. (2012)
ϵ	Bulk modulus of elasticity	MPa	Change in pressure potential per change in symplastic water content; higher values (less elastic leaves) related to sclerophylly	Bartlett, Scoffoni, et al. (2012)
f_{apo}	Fraction of apoplast water	unitless	Fraction of extracellular water content (non-symplastic water; in cell walls, xylem lumen)	Bartlett, Scoffoni, et al. (2012)
N_{os}/DM	number of osmoles per dry mass	mmol g ⁻¹	Number of active osmoles (solutes) contributing to π_0 normalised by leaf dry mass	Tyree and Jarvis (1982)
C_{ft}	Tissue-specific capacitance at full turgor	MPa ⁻¹	Change in relative water content per water potential change above the turgor loss point, or fraction of water mobilised under application of a pressure of 1 MPa; ‘capacitor’	Scoffoni et al. (2014); Xiong and Nadal (2020)
$C_{\text{ft, mass}}^*$	Leaf-specific capacitance at full turgor per dry mass	mmol g ⁻¹ MPa ⁻¹	C_{ft} normalised by leaf dry mass; absolute amount of water mobilised under 1 MPa; ‘bulk’ leaf capacitance	Blackman and Brodribb (2011); Scoffoni et al. (2014)
$C_{\text{ft, area}}^*$	Leaf-specific capacitance at full turgor per area	mol m ⁻² MPa ⁻¹	C_{ft} normalised by leaf area; related to leaf hydraulic conductance and stomatal response	Sack et al. (2003); Blackman and Brodribb (2011); Xiong and Nadal (2020)
RWC_{tlp}	Relative water content at the turgor loss point	%	RWC (volume) at the turgor loss or wilting point; partially determined by ϵ	Bartlett, Scoffoni, et al. (2012)

chemical basis of the proposed relationships, given the key role of cell walls and N content in driving photosynthetic capacity (Flexas et al., 2021; Onoda et al., 2017). Cell wall composition (pectin, hemicellulose and cellulose content) was also included in the analysis due to recent work highlighting its association to both photosynthesis and PV traits in response to water stress (Roig-Oliver et al., 2020, 2021).

MATERIALS AND METHODS

Data collection

In the present study, we use a combination of previously published data and newly measured plants from the UIB campus (Palma de Mallorca, Spain). The list of species is displayed in [Table S1](#). In some cases, plants growing

under different conditions (e.g. mature field plants versus potted plants grown outdoors or in a growth chamber) and/or displaying young and old leaves (in the case of some evergreens) were included for the same species. The complete dataset comprehends leaf photosynthesis, bulk structure, and PV measurements for a total of 45 data entries from 37 species. In addition, only for the 20 species included in the study of Nadal et al. (2018) (except *Nephrolepis exaltata*), we measured leaf anatomy, N and C content, and cell wall composition (see Methods S2 for technical details regarding these measurements).

Gas exchange

Measurements of plants from the UIB campus were conducted in June–July 2020. Mature individuals with no signs of stress were selected for the measurements. Branches were collected from the field at sunset, re-cut under water to avoid hydraulic failure, and measured the next day in a growth chamber (25–30°C, 40%–60% RH, 300–600 $\mu\text{mol m}^{-2} \text{s}^{-1}$ light intensity). Gas exchange was measured in four to six leaves from different individuals per species and conditions using an open gas exchange system with a coupled 2 or 6 cm^2 (depending on the species) fluorescence chamber (Li-6800; Li-Cor Inc.). Light-saturated net CO_2 assimilation per area ($A_{n,\text{area}}$) was recorded after reaching steady-state at ambient CO_2 (400 $\mu\text{mol mol}^{-1}$). All measurements were performed at 25°C block temperature, 1–2 kPa leaf VPD and $>1200 \mu\text{mol m}^{-2} \text{s}^{-1}$ PAR irradiance.

Pressure–volume curves

Parameters describing leaf water relations were obtained from PV curves conducted in leaves from the same branches collected for gas exchange. Individual leaves or branches (depending on if they were potted or field-sown plants) were rehydrated overnight with distilled water (using the ‘standing’ method of rehydration through the petiole in the case of individual leaves; Arndt et al., 2015). Measurements were performed in four to six leaves per species and conditions using the bench-dry method, where leaf mass and water potential (Ψ_{leaf} ; pressure chamber model 600D; PMS Instrument Company) are measured alternately in a dehydrating leaf. Following the protocol and calculations described by Sack and Pasquet-Kok (2011), we obtained the osmotic potential and relative water content at turgor loss point (π_{tlp} and RWC_{tlp} respectively), the osmotic potential at full turgor (π_o), the bulk modulus of elasticity calculated from the total water content (ϵ^*), the leaf saturated water content calculated from leaf weight when $\Psi_{\text{leaf}} = 0$ MPa (LSWC), the capacitance at full turgor (C_{ft}), and the leaf area-specific capacitance at full turgor ($C_{\text{ft,area}}^*$). Additionally, we calculated the fraction of apoplastic water (f_{apo}) as 1 – x -intercept in

the $-1/\Psi_{\text{leaf}}$ versus 100 – RWC relationship, and the bulk modulus of elasticity from the *symplast* water content (ϵ) as $\epsilon = \epsilon^* (1 - f_{\text{apo}})$ (Bartlett, Scoffoni, et al., 2012). The number of osmoles (N_o) was calculated as described from equation 3 following Tyree and Jarvis (1982). Any ‘plateau’ effect was discarded from the data points included in the calculations.

Leaf bulk structure

Leaf mass per area and its components were measured in leaves used for either gas exchange or for PV curves across the species included in the study following standardised protocols described by Pérez-Harguindeguy et al. (2013). Leaf thickness (LT) was estimated as the average of six measurements using a digital calliper (three measurements in *Olea europaea* and *Marsilea quadrifolia* due to their narrow and small leaves). Leaf area was analysed using the ImageJ software (Wayne Rasband/NIH). Leaf dry matter (DM) was obtained after >72 h at 70°C. Leaf density (LD) was then calculated as $\text{LD} = \text{LMA}/\text{LT}$. For most species included in the study, we also measured the saturated weight (SW) after rehydrating the leaves for ~ 24 h with distilled water in plastic bags at 4°C, thus allowing the calculation of ‘measured’ leaf saturated water content as $\text{LSWC} = (\text{SW} - \text{DM})/\text{DM}$. Mean LMA was used for converting area- to mass-based photosynthesis and capacitance ($A_{n,\text{mass}}$ and $C_{\text{ft, mass}}^*$ respectively).

Statistical analysis

Unless indicated otherwise, \log_{10} -transformation was applied to means ($n = 4–6$) per species and conditions for all statistical analyses. Data for the same species under different conditions were considered as independent data points, as in Sack et al. (2003). Analyses were performed using the R statistical software (R version 4.2.0; R Core Team, 2022). Relationships among parameters were quantified using standardised major axis slopes (SMA) and Pearson correlations. The *sma* function from the ‘SMATR’ package (Warton et al., 2012) was used for SMA fittings and *rcorr* from the ‘Hmisc’ package (Harrell Jr, 2022) for correlations. To discern direct versus indirect relationships, path model analyses were conducted through structural equation modelling (SEM) using the *sem* function from the ‘LAVAN’ package (Rosseel, 2012) on standardised data means using the *scale* function (R Core Team, 2022). A priori models were constructed following the theoretical framework displayed in Box 1. Principal component analysis (PCA) was conducted on standardised data using the function *prcomp* in the ‘STATS’ package (R Core Team, 2022); principal components and their loadings were plotted using the ‘FACTOEXTRA’ package (Kassambara & Mundt, 2020).

BOX 1 Theory relating LMA components to photosynthesis and PV traits

Net CO₂ assimilation on a mass basis ($A_{n,\text{mass}}$) can be formulated in terms of assimilation expressed on an area basis ($A_{n,\text{area}}$) and leaf mass per area (LMA), the latter resulting from a combination of leaf thickness (LT) and density (LD); hence:

$$A_{n,\text{mass}} = \frac{A_{n,\text{area}}}{\text{LMA}} = \frac{A_{n,\text{area}}}{\text{LT} \times \text{LD}} \quad (1)$$

LD is defined as dry matter (DM) per leaf volume (LV) at full turgor (Witkowski & Lamont, 1991). LV can be considered as the sum of the saturated water (V_{sw}), dry matter (V_{dm}) and air (V_{air}) volumetric fractions of the leaf (see similar approaches in Roderick, Berry, Noble, et al., 1999; Shipley et al., 2006). When the specific density of the non-gaseous fractions is included, then LD can be directly related to leaf saturated water content (LSWC; g H₂O g⁻¹ DM) as:

$$\text{LD} = \frac{\text{DM}}{\text{LV}} = \frac{\text{DM}}{V_{\text{sw}} + V_{\text{dm}} + V_{\text{air}}} = \frac{\text{DM}}{\text{SW}/\rho_{\text{w}} + \text{DM}/\rho_{\text{dm}} + V_{\text{air}}} = \frac{1}{\text{LSWC} + a} \quad (2)$$

being SW the saturated water mass, ρ_{w} the specific density of water (1 g cm⁻³), and ρ_{dm} the specific density of the dry matter. The final term a corresponds to $1/\rho_{\text{dm}} + V_{\text{air}}/\text{DM}$. Tyree and Jarvis (1982) defined the leaf osmotic potential at full turgor (π_{o}) for non-ideal solutions as the number of osmoles (N_{os}) per water mass in the symplast at saturation (SW_{sym}). If N_{os} is defined in terms of leaf dry matter (N_{os}/DM ; Kwon & Pallardy, 1989), then LSWC can be included in the formula:

$$\pi_{\text{o}} = \frac{-R \times T \times \rho_{\text{w}} \times N_{\text{os}}}{\text{SW}_{\text{sym}}} = \frac{-R \times T \times \rho_{\text{w}} \times N_{\text{os}}/\text{DM}}{\text{SW}_{\text{sym}}/\text{DM}} = \frac{-R \times T \times \rho_{\text{w}} \times N_{\text{os}}/\text{DM}}{\text{LSWC} \times (1 - f_{\text{apo}})} \quad (3)$$

where R is the gas constant (8.134 m³ Pa K⁻¹ mol⁻¹), T is the temperature (25°C) and f_{apo} is the fraction of water in the apoplast. Equation (3) shows a possible relationship between one of the components of LMA (LD through LSWC) with one of the key PV traits, since π_{o} is the main determinant of water (or osmotic) potential at the turgor loss point (π_{tlp} ; Bartlett, Scoffoni, et al., 2012). The other PV parameter that can be linked to the components of LMA is leaf-specific capacitance at full turgor (C_{ft}^*), since water storage (defined by LSWC) is one of the components of C_{ft}^* (Sack & Tyree, 2005; Scoffoni et al., 2014). Indeed, LSWC is directly related to leaf-specific capacitance at full turgor when expressed in absolute terms and normalised by dry mass ($C_{\text{ft,mass}}^*$), equivalent to the 'bulk' capacitance defined by Blackman and Brodribb (2011):

$$C_{\text{ft,mass}}^* = \frac{\Delta \text{RWC}}{\Delta \Psi} \times \frac{\text{SW}}{\text{DM}} = C_{\text{ft}} \times \text{LSWC} \quad (4)$$

where C_{ft} is the tissue-specific leaf capacitance at full turgor, that is, the fraction of water storage above the turgor loss point (Bartlett, Scoffoni, et al., 2012; Scoffoni et al., 2014). $C_{\text{ft,mass}}^*$ is expressed in mmol of H₂O when accounting for the molar mass of water (Blackman & Brodribb, 2011). Note that $C_{\text{ft,area}}^*$ is $C_{\text{ft,mass}}^* \times \text{LMA}$. According to the formulation of Bartlett, Scoffoni, et al. (2012), C_{ft} depends on f_{apo} , π_{o} and the bulk modulus of elasticity derived from the symplast water content (ϵ), since these are the parameters describing RWC_{tlp} and π_{tlp} :

$$C_{\text{ft}} = \frac{1 - \text{RWC}_{\text{tlp}}/100}{-\pi_{\text{tlp}}} = \frac{(1 - f_{\text{apo}}) \times (\pi_{\text{o}} + \epsilon)}{\epsilon^2} \quad (5)$$

Equations (1), (3) and (4) point towards a potential central role of LD and LSWC in linking photosynthesis with π_{o} and capacitance. In turn, LD and LSWC are inversely proportional (Equation 2), although their exact relationship may depend on the nature of the leaf dry matter (ρ_{dm}) and leaf air spaces. Equation (2) differs from previous similar attempts of linking leaf structure with leaf water content (Roderick, Berry, Noble, et al., 1999; Shipley et al., 2006; Vile et al., 2005) in that the leaf dry and water fractions are separated, thus allowing the connection between LMA components and PV-derived parameters.

For the main parameters included in the theoretical framework (Box 1), the relative contribution of the variables determining them was calculated following the variance partitioning approach of Onoda et al. (2011), given that $A_{n,mass}$, π_o , C_{ft} and $C_{ft,mass}^*$ are defined in an exact manner (no error term) from their respective components (Equations 1, 3–5). For these parameters, the variance of parameter Y equals the sum of its covariance with each of its X_i components: $\text{Var}(Y) = \text{Cov}(Y, X_1) + \text{Cov}(Y, X_2) + \dots + \text{Cov}(Y, X_i)$. The relative contribution of X_i to the variation of Y can thus be calculated as $|\text{Cov}(Y, X_i)|/\text{Var}(Y)$. For performing this analysis, eqns. shown in Box 1 need to display the structure $Y = X_1 + X_2 + \dots + X_i$; thus, Equations (1), (3)–(5) where log-transformed (see the resulting equations in Methods S1). We used calculated C_{ft} and $C_{ft,mass}^*$ using Equations (4) and (5) (Bartlett, Scoffoni, et al., 2012) for this analysis instead of the measured values from PV curves (Sack & Pasquet-Kok, 2011) for producing exact relationships for the equations describing C_{ft} and $C_{ft,mass}^*$. Nonetheless, the resulting contributions for these parameters are reliable since the calculated values were almost identical to the measured ones ($r > 0.99$ for both).

RESULTS

Across the included species, $A_{n,area}$ varied 6-fold (from 5.5 in *Nephrolepis exaltata* to 32.8 $\mu\text{mol m}^{-2} \text{s}^{-1}$ in *Helianthus annuus*) and LMA varied 15-fold (from 13.2 in *Phaseolus vulgaris* to 205 g m^{-2} in *Arbutus unedo*). This range in the two parameters resulted in a 23-fold variation in $A_{n,mass}$ (36–839 $\text{nmol g}^{-1} \text{s}^{-1}$). LMA was related to both LT and LD, being the latter the stronger driver of LMA ($R^2 = 0.53$; Figure S1). LT and LD displayed a similar range of variation (8- and 11-fold respectively), although they varied independently of each other ($p = 0.10$; Figure S1). Notably, the resurrection plant *Craterostigma plantagineum* presented significantly higher LT (0.87 mm) compared to the rest of species included in the study (Figure S1). LT values obtained using the digital calliper were strongly correlated with the thickness from anatomical sample analysis using light microscopy ($r^2 = 0.88$ for linear fit; Figure S2), supporting the reliability of our LD estimation. As predicted by theory (Equation 2), LD and LSWC showed a strong inverse relationship across species (Figure 1). Regarding PV traits, π_{tlp} varied 4-fold (from -0.64 in *Solanum lycopersicum* to -2.67 MPa in *Quercus ilex*) and was mainly determined by π_o ($R^2 = 0.93$; $p < 0.001$), and only weakly related to ε ($R^2 = 0.34$; $p < 0.001$). On the other hand, ε was the main parameter from Equation (5) driving changes in C_{ft} ($R^2 = 0.30$; $p < 0.001$; Table S2). C_{ft} is the parameter related the most to RWC_{tlp} (Table S2) and is a strong driver of both $C_{ft,area}^*$ and $C_{ft,mass}^*$ (Table S2), which presented 20- and 54-fold variation respectively. For $C_{ft,mass}^*$ values ranged from 1.4 in *Ficus nitida* to 76.3 $\text{mmol g}^{-1} \text{MPa}^{-1}$ in *C. plantagineum*.

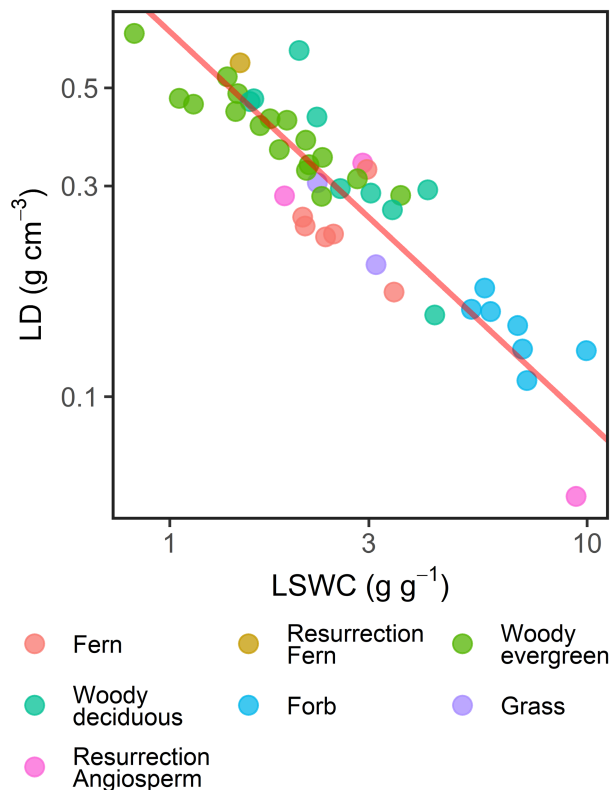


FIGURE 1 Relationship between leaf saturated water content (LSWC) and density (LD). Significant SMA fit ($R^2 = 0.822$, $p < 0.001$) denoted by red line. Circles represent mean for each species and condition. LSWC values correspond to the obtained from PV curves.

The relationships between leaf structure and photosynthesis and PV traits were considered on the same basis of expression, that is, parameters were compared on either an area or a mass basis. Following this rationale and the theoretical framework presented in Box 1, $A_{n,area}$ and $C_{ft,area}^*$ were compared to LMA and $A_{n,mass}$ and $C_{ft,mass}^*$ to LSWC (Figure 2). LMA was not related to area-based A_n and leaf specific capacitance, and only weakly related to π_{tlp} (Figure 2a–c). On the other hand, mass-based A_n and specific capacitance increased with higher LSWC (Figure 2d,e). π_{tlp} showed a stronger relationship with LSWC than with LMA ($R^2 = 0.45$ and 0.18, respectively); and leaves with higher water content presented higher (less negative) π_o and π_{tlp} (Figure 2f; Table S2). Unsurprisingly, this common coordination with LSWC resulted in the scaling of $A_{n,mass}$ with $C_{ft,mass}^*$ (Figure 3a) and its negative relationship with π_{tlp} (Figure 3b). Similarly, π_{tlp} was lower (more negative) in denser leaves (Figure 3c), although the relationship of π_{tlp} with LD was weaker than that with LSWC ($R^2 = 0.32$ and 0.45, respectively). The nature of the coordination between $A_{n,mass}$ and $C_{ft,mass}^*$ was explored using path analysis, which showed that leaf capacitance had little direct effect on A_n , and that LSWC was directly driving both $A_{n,mass}$ and $C_{ft,mass}^*$ (Figure S3a). The coordination between $A_{n,mass}$ and π_{tlp} followed the same pattern, being LSWC the direct determinant of both (Figure S3b).

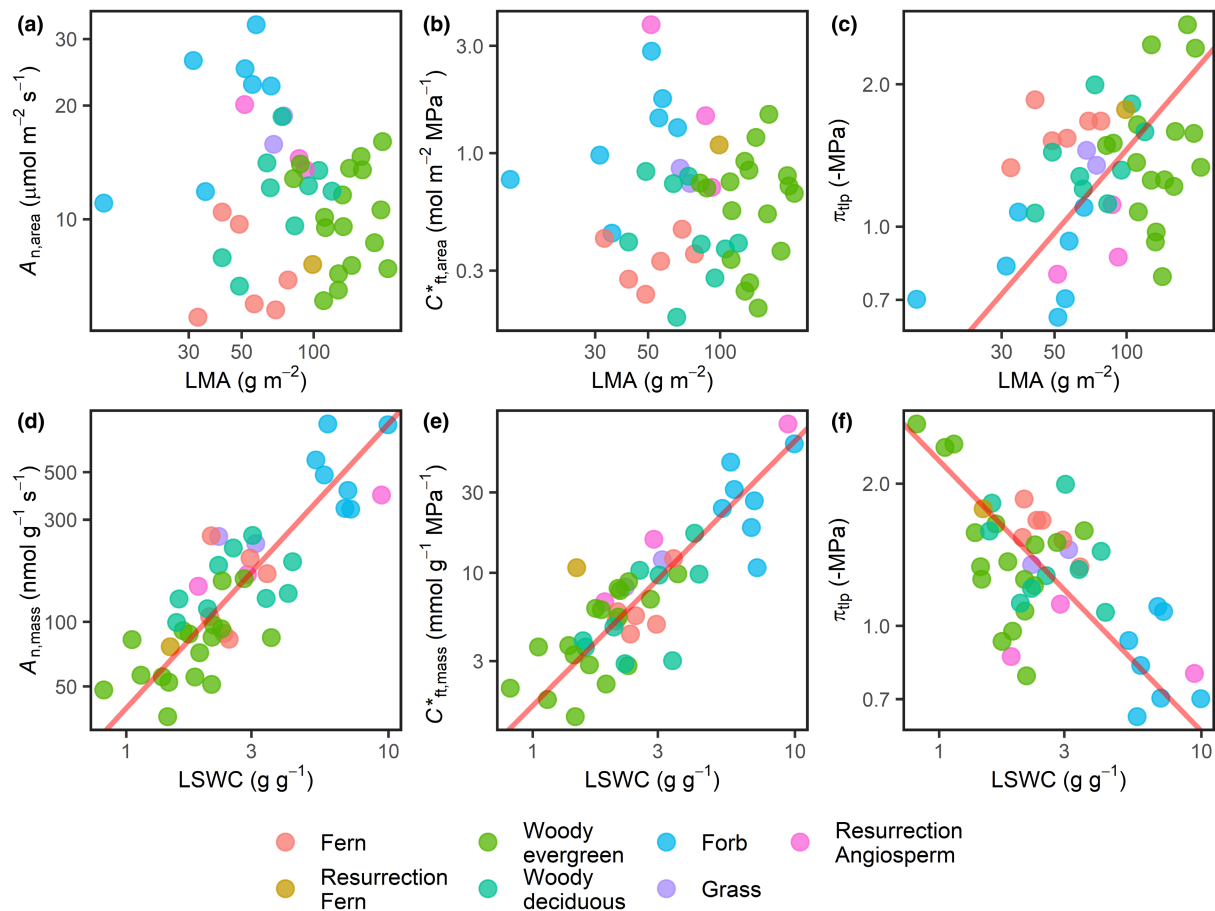


FIGURE 2 Coordination among area- and mass-based photosynthesis, structural and PV traits. Leaf mass per area (LMA) and area-based net CO₂ assimilation ($A_{n,area}$; a), no significant SMA fit ($R^2 = 0.024$, $P = 0.311$). LMA and leaf area-specific capacitance at full turgor ($C_{ft,area}^*$; b), no significant SMA fit ($R^2 = 0.009$, $p = 0.524$). LMA and osmotic potential at turgor loss point (π_{tlp} ; c), significant SMA fit ($R^2 = 0.175$, $p = 0.004$). Leaf saturated water content (LSWC) and mass-based net CO₂ assimilation ($A_{n,mass}$; d), significant SMA fit ($R^2 = 0.701$, $p < 0.001$). LSWC and leaf mass-specific capacitance at full turgor ($C_{ft,mass}^*$; e), significant SMA fit ($R^2 = 0.711$, $p < 0.001$). LSWC and π_{tlp} (d), significant SMA fit ($R^2 = 0.446$, $p < 0.001$). Circles represent mean for each species and condition. LSWC values correspond to the obtained from PV curves.

The trait framework displayed in Figure 4a summarises the main relationships found among photosynthesis, leaf structure and PV traits. The connections established between parameters are based on the theory that underpins them (Box 1) and the empirical relationships described above. LSWC contributes to ~50% of the explained variance for both $A_{n,mass}$ (through its effects on LD and LMA) and $C_{ft,mass}^*$, and to ~40% for π_o . The remaining ~50% of the variance of $A_{n,mass}$ and $C_{ft,mass}^*$ is explained mainly by $A_{n,area}$ and ϵ (the main driver of C_{ft}). A PCA was conducted (Figure 4b,c) to discern if there is a common axis of variation among the studied leaf traits. Indeed, $C_{ft,mass}^*$, LSWC, $A_{n,mass}$, LD, LMA and π_{tlp} were strongly associated with PC1 (47% variance explained; Figure 4b, Figure S4), which also partially included π_o . PC2 (23% variance) was mainly driven by N_{os}/DM , f_{apo} and ϵ , with minor contribution of π_o (Figure 4b, Figure S4). Notably, $A_{n,area}$ and LT (and, to a lesser extent, C_{ft}) were the most independent variables (i.e. the ones not related with neither PC1 nor PC2) among the set of variables in this study (Figure S4). Growth forms were

differentiated along PC1, since the forbs included in the study presented the higher $C_{ft,mass}^*$, LSWC and $A_{n,mass}$ compared to the rest of species, whereas the woody evergreen species occupied the other extreme of the axis (Figure 4c).

From the trait framework analysis and PCA, LSWC was identified as the key variable driving most trait variation. Thus, we explored its possible anatomical and chemical determinants in the Nadal et al. (2018) subset. Among the analysed parameters, LSWC was only related to cell dimensions and to carbon and nitrogen content (Table S3). LSWC escalated with cross-section cell area (a proxy to cell size), primarily of mesophyll (Figure S5a) but also of epidermis cells (Figure S5b); on the other hand, LSWC showed a strong inverse relationship with C per dry mass (Figure S5c) and a weaker, positive relationship with N per dry mass (Figure S5d). No relationship was found for cell wall composition (fraction of celluloses, hemicelluloses and pectins) with LSWC (Table S3). Notably, mesophyll cell wall thickness was not related to either

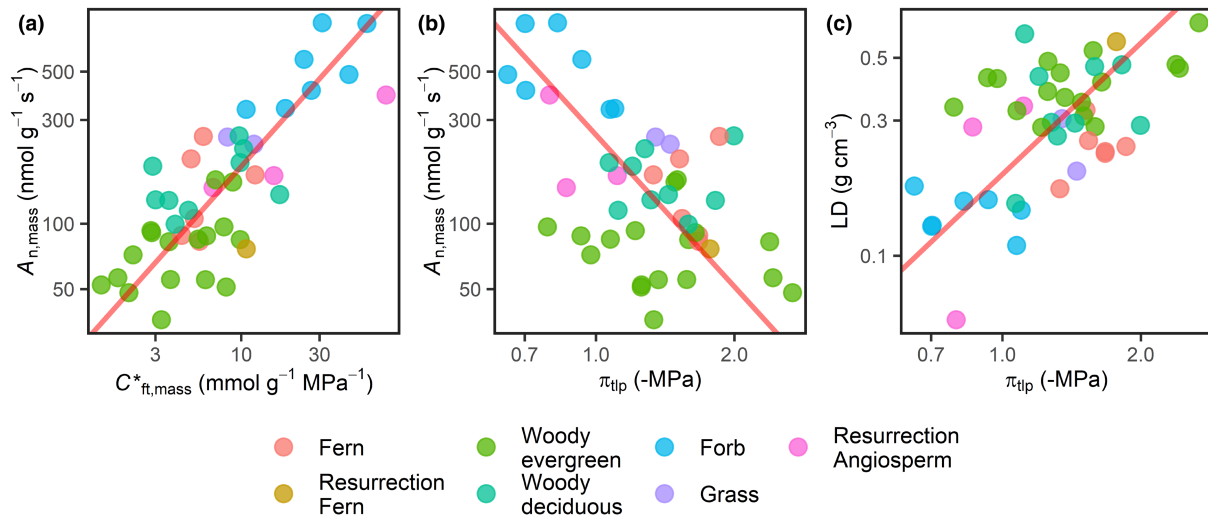


FIGURE 3 Relationship between leaf photosynthesis, density and PV traits. Net CO₂ assimilation on a mass basis ($A_{n, \text{mass}}$) and leaf mass-specific capacitance at full turgor ($C_{\text{ft, mass}}^*$; a), significant SMA fit ($R^2 = 0.625$, $p < 0.001$). $A_{n, \text{mass}}$ and osmotic potential at turgor loss point (π_{tlp} ; b), significant SMA fit ($R^2 = 0.303$, $p < 0.001$). Leaf density (LD) and π_{tlp} (c), significant SMA fit ($R^2 = 0.317$, $p < 0.001$). Circles represent mean for each species and condition.

$A_{n, \text{area}}$ or ϵ (Table S3), whereas ϵ showed a positive relationship with the N:C ratio (Table S3).

DISCUSSION

The present study expands on the previous work presented in Nadal et al. (2018) and Xiong and Nadal (2020), and establishes a central role of the water content per dry matter in determining the link between carbon economics and water relations in leaves. Our dataset covers a significant portion of trait variation; the ranges of LMA, LT and LD are approximately within the fifth and 95th percentiles of their respective range of values as compiled by Hodgson et al. (2011) for ~2000 species. Similarly, data for A_n and ϵ cover the range of the values reported for the studied groups (Bartlett, Scoffoni, et al., 2012; Flexas & Carricú, 2020); in the case of π_{tlp} , our results fall within the values described by Bartlett, Scoffoni, et al. (2012) for non-desert species. The studied species include ferns and resurrection (desiccation-tolerant) plants in addition to woody and herbaceous angiosperms, so we considered disparate growth forms and strategies. Hence, we are confident regarding the representativeness of the studied leaf traits.

Our results show how $A_{n, \text{mass}}$, $C_{\text{ft, mass}}^*$ and π_{tlp} , shared a common axis of variation (Figures 3a,b and 4a,b), which is driven by the close relationship between LD and LSWC (Figure 1) and their association with $A_{n, \text{mass}}$ and LMA, and $C_{\text{ft, mass}}^*$ and π_{tlp} respectively (Box 1, Figure 4a). The strong correlation between LD and LSWC was predicted by the theory (Equation 2) and supported by numerous reports relating leaf volume to water content (Castro-Diez et al., 2000; Hodgson et al., 2011; Niinemets, 1999; Pyankov et al., 1999; Shipley & Vu, 2002; Vile et al., 2005). The air volume fraction

accounts for a significant portion of the unexplained variance (~25%) between the two traits. Nonetheless, the air fraction is unlikely to affect water relations; accordingly, LSWC is more strongly related to other PV parameters than LD is (Table S2), thus supporting the overall framework displayed in Figure 4a. This also explains the higher R^2 of π_{tlp} with LSWC compared to LMA (0.45 and 0.18 respectively; Figure 2c,f), since the later includes leaf thickness and the air fraction (Box 1). Such pattern is found in other studies considering either LD or water content (Bartlett, Scoffoni, Ardy, et al., 2012; Fu et al., 2012; Ishida et al., 2008; Liu & Osborne, 2015; Méndez-Alonzo et al., 2019), partially due to the lack of correlation between π_{tlp} and LT (Table S2). The association of π_{tlp} with photosynthesis and structure was weaker than for the other variables (Figures 2 and 3), since a significant portion of the variation in π_o (and thus π_{tlp}) was captured by f_{apo} and N_o/DM , which were mostly independent from other traits (Figure 4, Figure S4). Nonetheless, our approach suggests that the association of π_{tlp} and LMA proposed by Zhu et al. (2018) results from LSWC rather than LMA directly affecting π_{tlp} .

A key relationship emerging among the set of leaf traits is the positive scaling between $A_{n, \text{mass}}$ and $C_{\text{ft, mass}}^*$ (Figure 3a). This relationship might be expected since both photosynthesis and capacitance are positively related to leaf hydraulics, namely K_{leaf} , due to the need for higher water transport and buffering capacity in leaves with high photosynthetic capacity—and thus elevated transpiration (Brodribb et al., 2007; Sack et al., 2003; Sack & Tyree, 2005; Xiong & Nadal, 2020). However, the path analysis (Figure S3a) shows that rather than one directly driving the other, this is an indirect relationship through the effect of LSWC on both $A_{n, \text{mass}}$ and $C_{\text{ft, mass}}^*$. LSWC is associated with ‘bulk’ rather than ‘dynamic’

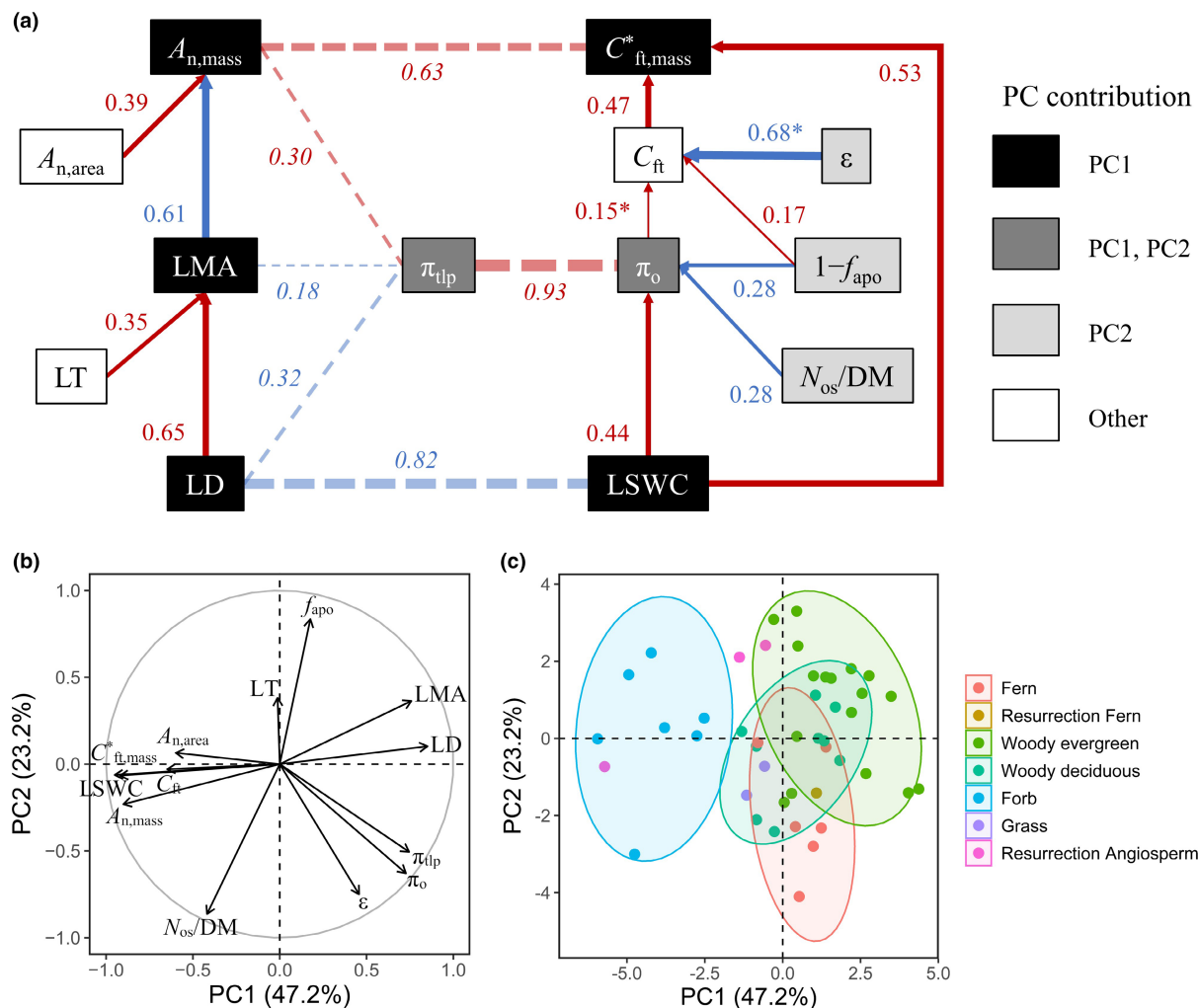


FIGURE 4 Multivariate analysis of leaf photosynthesis, structure and PV traits. A conceptual trait framework can be derived from the trait relationships described in Box 1 (a); the relative contributions from the partitioning of variance analysis are displayed as arrows and solid lines connecting the different parameters. These parameters are net CO₂ assimilation on a mass basis ($A_{n,mass}$), derived from area-based assimilation ($A_{n,area}$) and leaf mass per area (LMA), the latter defined by leaf thickness (LT) and density (LD); osmotic potential at full turgor (π_o), derived from leaf saturated water content (LSWC), the number of osmoles per dry matter (N_{os}/DM) and the fraction of apoplasmic water (f_{apo}); capacitance at full turgor (C_{ft}), derived from π_o , f_{apo} and the bulk modulus of elasticity from symplast water content (ϵ); and the leaf mass-specific capacitance at full turgor ($C_{ft,mass}^*$), derived from C_{ft} and LSWC. The equations for calculating the relative contributions are described in Methods S1. The '*' denotes split variance from the $\pi_o + \epsilon$ component in Equation (5) (Box 1). LSWC values correspond to the obtained from PV curves. Dashed lines and numbers (R^2) in italics refer to SMA fittings between the indicated variables, where no exact partition of variance is possible. The osmotic potential at turgor loss point (π_{tlp}) is only related to π_o since osmotic potential is its main driver (Bartlett, Scoffoni, et al., 2012). Positive and negative relationships are represented by red and blue lines/arrows, respectively. The contribution of each parameter to the two principal components (PC1 and PC2) from the PCA results is indicated by the colour of the boxes. Vectors (b) indicate variable loadings and circles (c) represent means for each species and condition. Growth forms that include ≥ 5 species are depicted by concentration ellipses (level set at 0.8 in the *fviz_pca_ind* function).

capacitance, being the latter involved in the water transport inside leaves (Blackman & Brodrigg, 2011); separating $C_{ft,mass}^*$ (which reflects bulk capacitance) into its components may help in discerning the degree of hydraulic compartmentalisation involved in the relationship between $A_{n,mass}$ and LSWC (Xiong & Nadal, 2020). On the other hand, few studies have explored the intrinsic mechanisms that drive the relationship between A_n and LSWC under non-stressed conditions. The scaling of photosynthesis with increasing water content (Figure 2d) may be due to photosynthesis rate per volume being relatively

conserved across species; indeed, some studies have argued for such expression—photosynthesis rate per volume or water content—given that living systems operate on the basis of product concentration (Garnier et al., 1999; Roderick, Berry, Noble, et al., 1999). A recent meta-analysis by Wang et al. (2022) also shows a positive correlation between photosynthesis and leaf water content across a wide range of ecosystems and plant functional types, which is attributed to a positive relationship between metabolic processes (i.e. photosynthesis) and water content (Huang et al., 2020).

The central role of LSWC supports the framework proposed by Shipley et al. (2006), which pointed towards a key role of water content—more precisely, cell volume per cell wall—in driving the coordination between $A_{n, \text{mass}}$, N_{mass} and LMA. Measuring cell and cell wall volumes is rather difficult; instead, we show a positive correlation between LSWC and cross-sectional cell area (Figure S5a,b), indicating that a high water content reflects larger cells (and hence increased cell volume per cell wall). This result is in accordance with previous studies relating cell dimensions to leaf density (Castro-Díez et al., 2000; Garnier & Laurent, 1994; Pyankov et al., 1999; Villar et al., 2013). Additionally, in larger cells, the proportion of cell wall in the total dry matter would be lower due to their increased volume per cell wall, thus explaining the lower C_{mass} and higher N_{mass} and N:C with increasing LSWC (Figure S5c,d, Table S3), as reported in Roderick, Berry, Saunders, et al. (1999). Hence, our findings support the central role of cell dimensions in explaining the trade-offs among the LES traits (Shipley et al., 2006). Nonetheless, it is worth noting that cell walls present an additional effect on area-based traits ($A_{n, \text{area}}$, LMA), given the greater presence of thicker cell walls in high LMA species and their effect on mesophyll conductance (g_m), thus potentially limiting CO_2 diffusion in leaves with reduced chloroplast exposition (Flexas et al., 2021; Nadal et al., 2021; Onoda et al., 2017; Peguero-Pina, Sisó, et al., 2017).

In Nadal et al. (2018), we suggested that cell wall thickness (reflected by g_m and diffusion limitations) could constitute a common basis for the relationship between elasticity and photosynthesis; however, here we show that the relationship between ϵ and $A_{n, \text{area}}$ is not at the basis of the proposed coordination (in fact $A_{n, \text{area}}$ and ϵ vary independently in this extended dataset; Figure S4a, Table S2), and that ϵ is contributing directly only to capacitance (Figure 4a). Neither ϵ nor $A_{n, \text{area}}$ were related to mesophyll cell wall thickness (Table S3), despite theory relating wall thickness with the mechanical properties of single cells (Tyree & Jarvis, 1982), and some previous data in oaks (Peguero-Pina, Sancho-Knapik, et al., 2017). The lack of relationship between $A_{n, \text{area}}$ and cell wall thickness may be expected in relatively small datasets with limited thickness range (here, 0.1–0.6 μm ; see Flexas et al., 2021). The fact that N:C was related to ϵ (Table S3), where leaves with a higher N proportion are more elastic, indicates a potential subsidiary association between photosynthesis and ϵ , given the N requirements of photosynthesis and the trade-off in N allocation between the cell walls and the photosynthetic apparatus (Onoda et al., 2017). Few studies have considered N content as a driver of leaf elasticity (e.g. Onoda et al., 2008); further exploration of the role of N-rich components in cell walls is required to discern the basis of ϵ . Nonetheless, ϵ is independent of the other variables captured by the PC1 (Figure 4b, Figure S4), and so any potential association with A_n would come second to that of photosynthesis with LSWC and capacitance.

Overall, the theory and results presented here provide a basis for the coordination between leaf photosynthesis and structure with water relations derived from PV traits, with the saturated water content of leaves playing a central role: on the one hand, LSWC determines the coordination between $A_{n, \text{mass}}$, $C_{\text{ft, mass}}^*$ and π_{tip} , and, on the other hand, it constitutes a direct link to LMA through LD. Such central role of LSWC has been recently acknowledged by Wang et al. (2022), where the coordination of $A_{n, \text{mass}}$ and leaf water content is extended to the global level. In our dataset, $A_{n, \text{mass}}$ and not $A_{n, \text{area}}$ displayed the most significant associations with the other leaf traits (Figures 2 and 4, Figure S4). Hence, the relationships established here are more in line with an ‘investment and return’ perspective of leaf function, which is provided by considering traits on a mass basis (Westoby et al., 2013). In effect, not only $A_{n, \text{mass}}$ (contrary to $A_{n, \text{area}}$) is tightly coordinated with leaf lifespan (Onoda & Wright, 2018; Wright et al., 2004); water content is also related to leaf lifespan (Garnier & Navas, 2012; Ishida et al., 2008; Ryser, 1996; Ryser & Urbas, 2000). Given that PV traits are usually thought in terms of drought tolerance (Bartlett, Scoffoni, et al., 2012; Niinemets, 2001), their closer association with other traits directly related to the economy of leaves can be expected. Notably, our approach confers a relatively diminished role to LMA, given that $A_{n, \text{mass}}$ can be directly related to LSWC, and emphasises the water content in leaves as the main explanatory variable. Note that LSWC is the inverse of leaf dry matter content (LDMC) or the ratio of dry matter per saturated weight (Pérez-Harguindeguy et al., 2013), since $\text{LDMC} = 1/(\text{LSWC} + 1)$. This is a parameter often highlighted as a better predictor of leaf performance in response to various biotic and abiotic factors (Hodgson et al., 2011; Kazakou et al., 2009; Laughlin et al., 2010; Pontes et al., 2007; Queded et al., 2007; Roche et al., 2004; Rusch et al., 2009; Schädler et al., 2003; Smart et al., 2017; Wang et al., 2022; Wilson et al., 1999; Witkowski & Lamont, 1991), and even more reliable than LMA when intending to capture spatiotemporal variations among species (Garnier et al., 2001). However, LMA is still predominant in the literature, partially due to ‘historical inertia’ (Hodgson et al., 2011); on the other hand, we argue that LSWC (or LDMC) reflects the link between leaf structure and function more accurately than LMA, given its stronger relationship with photosynthesis and PV traits. Since LSWC measured from rehydrated leaves compares remarkably well to that obtained from PV curves (Figure S6) and this is a relatively easy-to-measure parameter (Pérez-Harguindeguy et al., 2013; Smart et al., 2017; Vaieretti et al., 2007), we strongly recommend using LSWC in future ecophysiological studies aiming to explore leaf and plant functional traits.

AUTHOR CONTRIBUTIONS

Miquel Nadal, Javier Gulías and Jaume Flexas planned the research; Miquel Nadal, María J. Clemente-Moreno, Margalida Roig-Oliver and Alicia V. Perera-Castro

performed the measurements; Miquel Nadal, Jaume Flexas and Yusuke Onoda developed the theoretical framework; Miquel Nadal analysed the data and drafted the manuscript. All authors contributed to subsequent revisions and discussion.

ACKNOWLEDGEMENTS

This work was supported by the project PGC2018-093824-B-C41 from the Ministerio de Ciencia, Innovación y Universidades (Spain) and the European Regional Development Fund (ERDF). MN was supported pre-doctoral fellowship BES-2015-072578, financed by the Ministerio de Economía y Competitividad (MINECO) and the European Social Fund; and postdoctoral fellowship Juan de la Cierva-Formación (FJC2020-043902-I), financed by MCIN/AEI/10.13039/501100011033 (Spain) and the European Union (‘NextGenerationEU/PRTR’). AVP-C was supported by the Ministerio de Educación, Cultura y Deporte (pre-doctoral fellowship FPU-02054). MR-O was supported by the MINECO, pre-doctoral fellowship FPU16/01544. YO was supported by grant JSPS KAKENHI #21H02564 (Japan). We thank the technical support for microscopy preparation provided by the Universitat de València (Secció de Microscopia Electrònica, SCSIE), Universidad de Murcia (Servicio de Apoyo a las Ciencias Experimentales) and Dr. Ferran Hierro (UIB, Serveis Científicotècnics), and CEBAS-CSIC (Murcia, Spain) Ionic Service for C and N quantification. We thank Dr. Eva Miedes (CBGP, UPM-INIA) for her help in cell wall composition analysis. We also thank Miquel Truyols and collaborators of the UIB Experimental Field and Glasshouses which are supported by the UIB Grant15/2015.

FUNDING INFORMATION

European Regional Development Fund, Grant/Award Number: PGC2018-093824-B-C41; European Social Fund, Grant/Award Number: BES-2015-072578; Japan Society for the Promotion of Science, Grant/Award Number: KAKENHI #21H02564; Ministerio de Ciencia e Innovación, Grant/Award Number: FJC2020-043902-I; Ministerio de Ciencia, Innovación y Universidades, Grant/Award Number: PGC2018-093824-B-C41; Ministerio de Economía y Competitividad, Grant/Award Number: BES-2015-072578FPU16/01544; Ministerio de Educación, Cultura y Deporte, Grant/Award Number: FPU-02054

CONFLICT OF INTEREST STATEMENT

None.

PEER REVIEW

The peer review history for this article is available at <https://publons.com/publon/10.1111/ele.14176>.

DATA AVAILABILITY STATEMENT

Data supporting the manuscript are available in the Dryad Digital Repository: <https://doi.org/10.5061/dryad.mgqnk993k>.

ORCID

Miquel Nadal  <https://orcid.org/0000-0003-1472-1792>

REFERENCES

- Arndt, S.K., Irawan, A. & Sanders, G.J. (2015) Apoplastic water fraction and rehydration techniques introduce significant errors in measurements of relative water content and osmotic potential in plant leaves. *Physiologia Plantarum*, 155, 355–368.
- Atkin, O.K., Bloomfield, K.J., Reich, P.B., Tjoelker, M.G., Asner, G.P., Bonal, D. et al. (2015) Global variability in leaf respiration in relation to climate, plant functional types and leaf traits. *The New Phytologist*, 206, 614–636.
- Bartlett, M.K., Klein, T., Jansen, S., Choat, B. & Sack, L. (2016) The correlations and sequence of plant stomatal, hydraulic, and wilting responses to drought. *Proceedings of the National Academy of Sciences of the United States of America*, 113(46), 13098–13103.
- Bartlett, M.K., Scoffoni, C., Ardy, R., Zhang, Y., Sun, S., Cao, K. et al. (2012) Rapid determination of comparative drought tolerance traits: using an osmometer to predict turgor loss point. *Methods in Ecology and Evolution*, 3, 880–888.
- Bartlett, M.K., Scoffoni, C. & Sack, L. (2012) The determinants of leaf turgor loss point and prediction of drought tolerance of species and biomes: a global meta-analysis. *Ecology Letters*, 15, 393–405.
- Blackman, C.J. & Brodribb, T.J. (2011) Two measures of leaf capacitance: insights into the water transport pathway and hydraulic conductance in leaves. *Functional Plant Biology*, 38, 118–126.
- Blonder, B., Violle, C., Bentley, L.P. & Enquist, B.J. (2011) Venation networks and the origin of the leaf economics spectrum. *Ecology Letters*, 14, 91–100.
- Brodribb, T.J., Field, T.S. & Jordan, G.J. (2007) Leaf maximum photosynthetic rate and venation are linked by hydraulics. *Plant Physiology*, 144, 1890–1898.
- Castro-Díez, P., Puyravaud, J.P. & Cornelissen, J.H.C. (2000) Leaf structure and anatomy as related to leaf mass per area variation in seedlings of a wide range of woody plant species and types. *Oecologia*, 124, 476–486.
- Cornwell, W.K., Cornelissen, J.H.C., Amatangelo, K., Dorrepaal, E., Eviner, V.T., Godoy, O. et al. (2008) Plant species traits are the predominant control on litter decomposition rates within biomes worldwide. *Ecology Letters*, 11, 1065–1071.
- Díaz, S., Kattge, J., Cornelissen, J.H.C., Wright, I.J., Lavorel, S., Dray, S. et al. (2016) The global spectrum of plant form and function. *Nature*, 529, 167–171.
- Flexas, J. & Carriqui, M. (2020) Photosynthesis and photosynthetic efficiencies along the terrestrial plant's phylogeny: lessons for improving crop photosynthesis. *The Plant Journal*, 101, 964–978.
- Flexas, J., Clemente-Moreno, M.J., Bota, J., Brodribb, T.J., Gago, J., Mizokami, Y. et al. (2021) Cell wall thickness and composition are involved in photosynthetic limitation. *Journal of Experimental Botany*, 72(11), 3971–3986.
- Flexas, J., Ribas-Carbó, M., Diaz-Espejo, A., Galmés, J. & Medrano, H. (2008) Mesophyll conductance to CO₂: current knowledge and future prospects. *Plant, Cell & Environment*, 31, 602–621.
- Flexas, J., Scoffoni, C., Gago, J. & Sack, L. (2013) Leaf mesophyll conductance and leaf hydraulic conductance: an introduction to their measurement and coordination. *Journal of Experimental Botany*, 64(13), 3965–3981.
- Fu, P.L., Jiang, Y.J., Wang, A.Y., Brodribb, T.J., Zhang, J.L., Zhu, S.D. et al. (2012) Stem hydraulic traits and leaf water-stress tolerance are co-ordinated with the leaf phenology of angiosperm trees in an Asian tropical dry karst forest. *Annals of Botany*, 110, 189–199.
- Garnier, E. & Laurent, G. (1994) Leaf anatomy, specific mass and water content in congeneric annual and perennial grass species. *New Phytologist*, 128(4), 725–736.

- Garnier, E., Laurent, G., Bellmann, A., Debain, S., Berthelot, P., Ducout, B. et al. (2001) Consistency of species ranking based on functional leaf traits. *The New Phytologist*, 152, 69–83.
- Garnier, E. & Navas, M.L. (2012) A trait-based approach to comparative functional plant ecology: concepts, methods and applications for agroecology. A review. *Agronomy for Sustainable Development*, 32, 365–399.
- Garnier, E., Salager, J.L., Laurent, G. & Sonié, L. (1999) Relationships between photosynthesis, nitrogen and leaf structure in 14 grass species and their dependence on the basis of expression. *The New Phytologist*, 143, 119–129.
- Harrell, F., Jr. (2022) *Hmisc: Harrell miscellaneous*. R Package Version 4.7-0. Available from: <https://CRAN.R-project.org/package=Hmisc>
- He, N., Li, Y., Liu, C., Xu, L., Li, M., Zhang, J. et al. (2020) Plant trait networks: improved resolution of the dimensionality of adaptation. *Trends in Ecology & Evolution*, 35(10), 908–918.
- He, P., Wright, I.J., Zhu, S., Onoda, Y., Liu, H., Li, R. et al. (2019) Leaf mechanical strength and photosynthetic capacity vary independently across 57 subtropical forest species with contrasting light requirements. *The New Phytologist*, 223(2), 607–618.
- Hikosaka, K. & Shigeno, A. (2009) The role of rubisco and cell walls in the interspecific variation in photosynthetic capacity. *Oecologia*, 160, 443–451.
- Hodgson, J.G., Monserrat-Martí, G., Charles, M., Jones, G., Wilson, P., Shipley, B. et al. (2011) Is leaf dry matter content a better predictor of soil fertility than specific leaf area? *Annals of Botany*, 108, 1337–1345.
- Huang, H., Ran, J., Ji, M., Wang, Z., Dong, L., Hu, W. et al. (2020) Water content quantitatively affects metabolic rates over the course of plant ontogeny. *The New Phytologist*, 228, 1524–1534.
- Ishida, A., Nakano, T., Yazaki, K., Matsuki, S., Koike, N., Lauenstein, D.L. et al. (2008) Coordination between leaf and stem traits related to leaf carbon gain and hydraulics across 32 drought-tolerant angiosperms. *Oecologia*, 156, 193–202.
- John, G.P., Henry, C. & Sack, L. (2018) Leaf rehydration capacity: associations with other indices of drought tolerance and environment. *Plant, Cell & Environment*, 41, 2638–2653.
- John, G.P., Scoffoni, C., Buckley, T.N., Villar, R., Poorter, H. & Sack, L. (2017) The anatomical and compositional basis of leaf mass per area. *Ecology Letters*, 20, 412–425.
- Kassambara, A. & Mundt, F. (2020) *Factoextra: extract and visualize the results of multivariate data analyses*. R Package Version 1.0.7. Available from: <https://CRAN.R-project.org/package=factoextra>
- Kattge, J., Bönsch, G., Díaz, S., Lavorel, S., Prentice, I.C., Leadley, P. et al. (2020) TRY plant trait database—enhanced coverage and open access. *Global Change Biology*, 26, 119–188.
- Kattge, J., Díaz, S., Lavorel, S., Prentice, I.C., Leadley, P., Bönsch, G. et al. (2011) TRY—a global database of plant traits. *Global Change Biology*, 17, 2905–2935.
- Kazakou, E., Violle, C., Roumet, C., Pintor, C., Gimenez, O. & Garnier, E. (2009) Litter quality and decomposability of species from a Mediterranean succession depend on leaf traits but not on nitrogen supply. *Annals of Botany*, 104, 1151–1161.
- Kitajima, K. & Poorter, L. (2010) Tissue-level leaf toughness, but not lamina thickness, predicts sapling leaf lifespan and shade tolerance of tropical tree species. *The New Phytologist*, 186, 708–721.
- Kwon, K.W. & Pallardy, S.G. (1989) Temporal changes in tissue water relations of seedlings of *Quercus acutissima*, *Q. alba*, and *Q. stellata* subjected to chronic water stress. *Canadian Journal of Forest Research*, 19(5), 622–626.
- Laughlin, D.C., Leppert, J.J., Moore, M.M. & Sieg, C.H. (2010) A multi-trait test of the leaf-height-seed plant strategy scheme with 133 species from a pine forest flora. *Functional Ecology*, 24, 493–501.
- Lenz, T.I., Wright, I.J. & Westoby, M. (2006) Interrelations among pressure-volume curve traits across species and water availability gradients. *Physiologia Plantarum*, 127, 423–433.
- Liu, H. & Osborne, C.P. (2015) Water relations traits of C_4 grasses depend on phylogenetic lineage, photosynthetic pathway, and habitat water availability. *Journal of Experimental Botany*, 66(3), 761–773.
- Lloyd, J., Bloomfield, K., Domingues, T.F. & Farquhar, G.D. (2013) Photosynthetically relevant foliar traits correlating better on a mass vs an area basis: of ecophysiological relevance or just a case of mathematical imperatives and statistical quicksand? *The New Phytologist*, 199, 311–321.
- Májeková, M., Hájek, T., Albert, A.J., de Bello, F., Doležal, J., Götzenberger, L. et al. (2021) Weak coordination between leaf drought tolerance and proxy traits in herbaceous plants. *Functional Ecology*, 35(6), 1299–1311.
- Maréchaux, I., Saint-André, L., Bartlett, M.K., Sack, L. & Chave, J. (2020) Leaf drought tolerance cannot be inferred from classic leaf traits in a tropical rainforest. *Journal of Ecology*, 108(3), 1030–1045.
- Martin-StPaul, N., Delzon, S. & Cochard, H. (2017) Plant resistance to drought depends on timely stomatal closure. *Ecology Letters*, 20(11), 1437–1447.
- Méndez-Alonso, R., Ewers, F.W., Jacobsen, A.L., Pratt, R.B., Scoffoni, C., Bartlett, M.K. et al. (2019) Covariation between leaf hydraulics and biomechanics is driven by leaf density in Mediterranean shrubs. *Trees*, 33, 507–519.
- Nadal, M., Flexas, J. & Gulias, J. (2018) Possible link between photosynthesis and leaf modulus of elasticity among vascular plants: a new player in leaf traits relationships? *Ecology Letters*, 21(9), 1372–1379.
- Nadal, M., Perera-Castro, A.V., Gulias, J., Farrant, J.M. & Flexas, J. (2021) Resurrection plants optimize photosynthesis despite very thick cell walls by means of chloroplast distribution. *Journal of Experimental Botany*, 72(7), 2600–2610.
- Niinemets, Ü. (1999) Components of leaf dry mass per area—thickness and density—alter leaf photosynthetic capacity in reverse directions in woody plants. *The New Phytologist*, 144, 35–47.
- Niinemets, Ü. (2001) Global-scale climatic controls of leaf dry mass per area, density, and thickness in trees and shrubs. *Ecology*, 82(2), 453–469.
- Niinemets, Ü., Diaz-Espejo, A., Flexas, J., Galmés, J. & Warren, C.R. (2009) Role of mesophyll diffusion conductance in constraining potential photosynthetic productivity in the field. *Journal of Experimental Botany*, 60, 2249–2270.
- Onoda, Y., Schieving, F. & Anten, N.P.R. (2008) Effects of light and nutrient availability on leaf mechanical properties of *Plantago major*: a conceptual approach. *Annals of Botany*, 101, 727–736.
- Onoda, Y., Westoby, M., Adler, P.B., Choong, A.M.F., Clissold, F.J., Cornelissen, J.H.C. et al. (2011) Global patterns of leaf mechanical properties. *Ecology Letters*, 14, 301–312.
- Onoda, Y. & Wright, I.J. (2018) The leaf economics spectrum and its underlying physiological and anatomical principles. In: Adams, W., III & Terashima, I. (Eds.) *The leaf: A platform for performing photosynthesis. Advances in photosynthesis and respiration*, Vol. 44. Cham: Springer, pp. 451–471.
- Onoda, Y., Wright, I.J., Evans, J.R., Hikosaka, K., Kitajima, K., Niinemets, Ü. et al. (2017) Physiological and structural tradeoffs underlying the leaf economics spectrum. *The New Phytologist*, 214, 1447–1463.
- Osnas, J.L.D., Lichstein, J.W., Reich, P.B. & Pacala, S.W. (2013) Global leaf traits relationships: mass, area, and the leaf economics spectrum. *Science*, 340, 741–744.
- Peguero-Pina, J.J., Sancho-Knapik, D. & Gil-Pelegrín, E. (2017) Ancient cell structural traits and photosynthesis in today's environment. *Journal of Experimental Botany*, 68, 1389–1392.
- Peguero-Pina, J.J., Sisó, S., Flexas, J., Galmés, J., García-Nogales, A., Niinemets, Ü. et al. (2017) Cell-level anatomical characteristics explain high mesophyll conductance and photosynthetic capacity in sclerophyllous Mediterranean oaks. *The New Phytologist*, 214(2), 585–596.

- Perera-Castro, A.V., Nadal, M. & Flexas, J. (2020) What drives photosynthesis during desiccation? Mosses and other outliers from the photosynthesis–elasticity trade-off. *Journal of Experimental Botany*, 71(20), 6460–6470.
- Pérez-Harguindeguy, N., Díaz, S., Garnier, E., Lavorel, S., Poorter, H., Jaureguiberry, P. et al. (2013) New handbook for standardised measurement of plant functional traits worldwide. *Australian Journal of Botany*, 61, 167–234.
- Pontes, L.D.S., Soussana, J.F., Louault, F., Andueza, D. & Carrère, P. (2007) Leaf traits affect the above-ground productivity and quality of pasture grasses. *Functional Ecology*, 21, 844–853.
- Poorter, H., Niinemets, Ü., Poorter, L., Wright, I.J. & Villar, R. (2009) Causes and consequences of variation in leaf mass per area (LMA): a meta-analysis. *The New Phytologist*, 182, 565–588.
- Pyankov, V.I., Kondratchuk, A.V. & Shipley, B. (1999) Leaf structure and specific leaf mass: the alpine desert plants of the eastern Pamirs, Tadjikistan. *New Phytologist*, 143, 131–142.
- Quested, H., Eriksson, O., Fortunel, C. & Garnier, E. (2007) Plant traits relate to whole-community litter quality and decomposition following land use change. *Functional Ecology*, 21, 1016–1026.
- R Core Team. (2022) *R: a language and environment for statistical computing*. Vienna, Austria: R Foundation for Statistical Computing. Available from: <https://www.R-project.org/>
- Read, J., Sanson, G.D., de Garine-Wichatitsky, M. & Jaffre, T. (2006) Sclerophylly in two contrasting tropical environments: low nutrients vs. low rainfall. *American Journal of Botany*, 93, 1601–1614.
- Reich, P.B. (2014) The world-wide ‘fast-slow’ plant economics spectrum: a traits manifesto. *Journal of Ecology*, 102, 275–301.
- Roche, P., Diaz-Burlinson, N. & Gachet, S. (2004) Congruency analysis of species ranking based on leaf traits: which traits are the more reliable? *Plant Ecology*, 174, 37–48.
- Roderick, M.L., Berry, S.L., Noble, I.R. & Farquhar, G.D. (1999) A theoretical approach to linking the composition and morphology with the function of leaves. *Functional Ecology*, 13, 683–695.
- Roderick, M.L., Berry, S.L., Saunders, A.R. & Noble, I.R. (1999) On the relationship between the composition, morphology and function of leaves. *Functional Ecology*, 13, 696–710.
- Roig-Oliver, M., Fullana-Pericàs, M., Bota, J. & Flexas, J. (2021) Adjustments in photosynthesis and leaf water relations are related to changes in cell wall composition in *Hordeum vulgare* and *Triticum aestivum* subjected to water deficit stress. *Plant Science*, 311, 111015.
- Roig-Oliver, M., Nadal, M., Clemente-Moreno, M.J., Bota, J. & Flexas, J. (2020) Cell wall components regulate photosynthesis and leaf water relations of *Vitis vinifera* cv. Grenache acclimated to contrasting environmental conditions. *Journal of Plant Physiology*, 244, 153084.
- Rossel, Y. (2012) Lavaan: an R package for structural equation modeling. *Journal of Statistical Software*, 48(2), 1–36.
- Rusch, G.M., Skarpe, C. & Halley, D.J. (2009) Plant traits link hypothesis about resource-use and response to herbivory. *Basic and Applied Ecology*, 10, 466–474.
- Ryser, P. (1996) The importance of tissue density for growth and life span of leaves and roots: a comparison of five ecologically contrasting grasses. *Functional Ecology*, 10, 717–723.
- Ryser, P. & Urbas, P. (2000) Ecological significance of leaf life span among central European grass species. *Oikos*, 91, 41–50.
- Sack, L., Cowan, P.D., Jaikumar, N. & Holbrook, N.M. (2003) The ‘hydrology’ of leaves: co-ordination of structure and function in temperate woody species. *Plant, Cell & Environment*, 26, 1343–1356.
- Sack, L., Pasquet-Kok, J. & PrometheusWiki Contributors. (2011) *Leaf pressure-volume curve parameters*. PrometheusWiki. Available from: <http://prometheuswiki.org/tiki-pagehistory.php?page=Leaf%20pressure-volume%20curve%20parameters&preview=16> [Accessed 10th April 2018].
- Sack, L., Scoffoni, C., John, G.P., Poorter, H., Mason, C.M., Mendez-Alonzo, R. et al. (2013) How do leaf veins influence the worldwide leaf economic spectrum? Review and synthesis. *Journal of Experimental Botany*, 64(13), 4053–4080.
- Sack, L. & Tyree, M.T. (2005) Leaf hydraulics and its implications in plant structure and function. In: Holbrook, N.M. & Zwieniecki, M.A. (Eds.) *Vascular transport in plants*. London (UK): Elsevier Academic Press, pp. 93–114.
- Salleo, S. & Nardini, A. (2000) Sclerophylly: evolutionary advantage or mere epiphenomenon? *Plant Biosyst*, 134, 247–259.
- Schädler, M., Jung, G., Auge, H. & Brandl, R. (2003) Palatability, decomposition and insect herbivory: patterns in a successional old-field plant community. *Oikos*, 103, 121–132.
- Scoffoni, C., Vuong, C., Diep, S., Cochard, H. & Sack, L. (2014) Leaf shrinkage with dehydration: coordination with hydraulic vulnerability and drought tolerance. *Plant Physiology*, 164, 1772–1788.
- Shipley, B., Lechowicz, M.J., Wright, I. & Reich, P.B. (2006) Fundamental trade-offs generating the worldwide leaf economics spectrum. *Ecology*, 87(3), 535–541.
- Shipley, B. & Vu, T.T. (2002) Dry matter content as a measure of dry matter concentration in plants and their parts. *The New Phytologist*, 153, 359–364.
- Smart, S.M., Glanville, H.C., Blanes, M.C., Mercado, L.M., Emmett, B.A., Jones, D.L. et al. (2017) Leaf dry matter content is better at predicting aboveground net primary production than specific leaf area. *Functional Ecology*, 31, 1336–1344.
- Tyree, M.T. & Jarvis, P.G. (1982) Water in tissues and cells. In: Lange, O.L., Nobel, P.S., Osmond, C.B. & Ziegler, H. (Eds.) *Physiological plant ecology II. Encyclopedia of plant physiology*, Vol. 12. Berlin, Heidelberg (Germany): Springer, pp. 35–77.
- Vaieretti, M.V., Díaz, S., Vile, D. & Garnier, E. (2007) Two measurement methods of leaf dry matter content produce similar results in a broad range of species. *Annals of Botany*, 99, 955–958.
- van Bodegom, P.M., Douma, J.C. & Verheijen, L.M. (2014) A fully traits-based approach to modeling global vegetation distribution. *Proceedings of the National Academy of Sciences of the United States of America*, 111, 13733–13738.
- Vile, D., Garnier, É., Shipley, B., Laurent, G., Navas, M.L., Roumet, C. et al. (2005) Specific leaf area and dry matter content estimate thickness in laminar leaves. *Annals of Botany*, 96, 1129–1136.
- Villar, R., Ruiz-Robledo, J., Uberta, J.L. & Poorter, H. (2013) Exploring variation in leaf mass per area (LMA) from leaf to cell: an anatomical analysis of 26 woody species. *American Journal of Botany*, 100(10), 1969–1980.
- Wang, Z., Huang, H., Wang, H., Peñuelas, J., Sardans, J., Niinemets, Ü. et al. (2022) Leaf water content contributes to global leaf trait relationships. *Nature Communications*, 13, 5525.
- Warton, D.I., Duursma, R.A., Falster, D.S. & Taskinen, S. (2012) Smatr 3—an R package for estimation and inference about allometric lines. *Methods in Ecology and Evolution*, 3(2), 257–259.
- Westoby, M., Reich, P.B. & Wright, I.J. (2013) Understanding ecological variation across species: area-based vs mass-based expression of leaf traits. *The New Phytologist*, 199, 322–323.
- Westoby, M. & Wright, I.J. (2006) Land-plant ecology on the basis of functional traits. *Trends in Ecology & Evolution*, 21(5), 261–268.
- Wilson, P.J., Thompson, K. & Hodgson, J.G. (1999) Specific leaf area and leaf dry matter content as alternative predictors of plant strategies. *The New Phytologist*, 143, 155–162.
- Witkowski, E.T.F. & Lamont, B.B. (1991) Leaf specific mass confounds leaf density and thickness. *Oecologia*, 88, 486–493.
- Wright, I.J., Reich, P.B., Westoby, M., Ackerly, D.D., Baruch, Z., Bongers, F. et al. (2004) The worldwide leaf economics spectrum. *Nature*, 428, 821–827.
- Xing, K., Niinemets, Ü., Rengel, Z., Onoda, Y., Xia, J., Chen, H.Y.H. et al. (2021) Global patterns of leaf construction traits and their covariation along climate and soil environmental gradients. *The New Phytologist*, 232, 1648–1660.
- Xiong, D. & Nadal, M. (2020) Linking water relations and hydraulics with photosynthesis. *The Plant Journal*, 101(4), 800–815.

Zhu, S.D., Chen, Y.J., Ye, Q., He, P.C., Liu, H., Li, R.H. et al. (2018) Leaf turgor loss point is correlated with drought tolerance and leaf carbon economics traits. *Tree Physiology*, 38, 658–663.

SUPPORTING INFORMATION

Additional supporting information can be found online in the Supporting Information section at the end of this article.

How to cite this article: Nadal, M., Clemente-Moreno, M.J., Perera-Castro, A.V., Roig-Oliver, M., Onoda, Y., Gulias, J. et al. (2023) Incorporating pressure–volume traits into the leaf economics spectrum. *Ecology Letters*, 26, 549–562. Available from: <https://doi.org/10.1111/ele.14176>